

# Technical Notes

## Shock-Tracking Procedure for Studying Screech-Induced Oscillations

Benoît André,\* Thomas Castelain,† and Christophe Bailly‡  
*Ecole Centrale de Lyon, 69134 Ecully Cedex, France*

DOI: 10.2514/1.J051057

### I. Introduction

**A** SHOCK-CONTAINING supersonic jet radiates two so-called shock-associated noise components in addition to the classical mixing noise. These two components are the broadband shock-associated noise and the screech. The latter was studied in the early 1950s by Powell [1]. Screech is a tonal noise component. Its generation mechanism has been explained with some success as a feedback loop involving sound production through shock-turbulence interaction. The broadband shock-associated noise component has been investigated at least since Martlew [2]. Harper-Bourne and Fisher [3] have adapted Powell's stationary source array model to derive some observed properties of this noise component. In his review about high-speed jet aeroacoustics, Seiner [4] points out the necessity of studying shock motion to confirm Powell's [1] model of stationary sources. Furthermore, fluid disturbances having a relative motion to shocks may be responsible for broadband shock noise [4]. A certain insight into shock behavior within a jet plume is thus essential to accurately understand shock-associated noise generation.

The screech phenomenon in a round jet involves different modes. They have been studied extensively in the past, for example, by Davies and Oldfield [5], Merle [6], or Powell et al. [7]. Mode switching appears as a sudden change of jet plume structure and screech frequency with operating conditions. Five modes are traditionally quoted: A1 and A2 are axisymmetric, B is sinuous or flapping, C is helical, and D is again sinuous. The reader is referred to Raman [8,9] for a review of screech properties.

The coincidence between shock oscillation frequency and screech frequency has been first observed by Lassiter and Hubbard [10] from a shadowgraph technique. Sherman et al. [11] have made use of high-speed schlieren recording to investigate the shock distortion during screech. They have also found the coincidence between oscillation and screech frequencies and estimated oscillation amplitudes for the third shock. Using an optical shock detection technique based on laser light scattering by a shock, Panda [12,13] has significantly contributed to the characterization of shock motion during screech. He has reported that every shock oscillates at the screech frequency

and motion amplitudes have been assessed. In the latter reference, an analytical model for shock oscillation is also proposed and is found to be in good agreement with measurements. To the authors' knowledge, Sherman et al.'s [11] and Panda's [12,13] contributions are the only occurrences of shock oscillation measurements in the screech literature.

In the present Note, oscillation frequency and amplitude are examined by means of high-speed schlieren images and simultaneous near-field acoustic recordings. A procedure for shock tracking is developed and applied on two different screech modes. The experimental setup is presented in Sec. II. The procedure is explained in Sec. III, and some results are discussed. Conclusions are finally given in Sec. IV.

### II. Experimental Setup

A 38-mm-diam contoured convergent nozzle is supplied by a compressor in unheated dry air, allowing continuous operation. The jet exhausts into the  $10 \times 8 \times 8$  m<sup>3</sup> anechoic chamber of the Centre Acoustique—Laboratoire de Mécanique des Fluides et d'Acoustique at École Centrale de Lyon. The stagnation pressure of the flow is controlled by an electrically driven valve and is measured downstream of it, along with stagnation temperature. In this Note, results obtained for the two values NPR = 2.27 and 2.54 are reported, where NPR denotes the nozzle pressure ratio. In these two cases, the measured NPR oscillates within 0.3% of the setpoint.

A conventional Z-type schlieren system is used to visualize the global structure of the choked jet. It consists of a fibered continuous QTH light source whose adjustable electrical power ranges up to 250 W and of two  $\lambda/8$ , 107.95-mm-diam, 863.6-mm-focal-length parabolic mirrors. The offaxis use of the mirrors is set to  $2\alpha = 10^\circ$ . A knife edge, set perpendicular to the jet axis, plays the role of the spatial filter. The schlieren images are recorded by a high-speed Phantom V12 CMOS camera whose frame rate is set to 20,000 Hz, with exposure time of 1  $\mu$ s. A 150-mm-focal-length lens is used to collimate the light beams on the camera sensor. According to this arrangement, the image resolution has been measured as 0.11 mm/pixel.

Near-field acoustic pressure measurements are performed with two 0.25 in. Brüel & Kjær 4939 microphones set in the nozzle exit plane, one nozzle diameter away from the jet centerline and  $180^\circ$  apart from each other. The measured signals are sampled at 102,400 Hz using a National Instruments PXI 5733 board.

A trigger common to schlieren and acoustic recordings is provided by the PXI acquisition card. This allows the video recording to be a posteriori linked to the emitted sound, which is the basis of the hereafter presented results. However, it has to be emphasized that no microphone-conditioned trigger has been implemented.

### III. Shock Motion Features

The existence of screech modes has already been mentioned. Shock oscillations are symmetric or antisymmetric about the jet centerline if the mode is symmetric or antisymmetric, respectively. Similarly, two diametrically opposed microphones in the near field will exhibit in-phase or out-of-phase signals in the two same cases. This latter property is clearly visible in Fig. 1. It is inferred that the NPR = 2.27 value corresponds to mode A and that the NPR = 2.54 value corresponds to mode B, which is in accordance with existing experimental data, for instance, in Powell et al. [7].

To reach some quantitative results about both frequency and amplitude of shock oscillation, the schlieren pictures have been pretreated before applying a shock-tracking algorithm. The pretreatment as well as a simplified sketch of the algorithm are shown in

Received 16 November 2010; revision received 1 March 2011; accepted for publication 1 March 2011. Copyright © 2011 by the authors. Published by the American Institute of Aeronautics and Astronautics, Inc., with permission. Copies of this paper may be made for personal or internal use, on condition that the copier pay the \$10.00 per-copy fee to the Copyright Clearance Center, Inc., 222 Rosewood Drive, Danvers, MA 01923; include the code 0001-1452/11 and \$10.00 in correspondence with the CCC.

\*Ph.D. Student, Université de Lyon, Laboratoire de Mécanique des Fluides et d'Acoustique, UMR CNRS 5509, 36 Avenue Guy de Collongue; benoit.andre@ec-lyon.fr.

†Assistant Professor, Université Lyon 1, 43 Boulevard du 11 Novembre 1918, 69622 Villeurbanne Cedex; Laboratoire de Mécanique des Fluides et d'Acoustique, UMR CNRS 5509.

‡Professor, Université de Lyon, Laboratoire de Mécanique des Fluides et d'Acoustique, UMR CNRS 5509, 36 Avenue Guy de Collongue; Institut Universitaire de France, Paris, France. Senior Member AIAA.

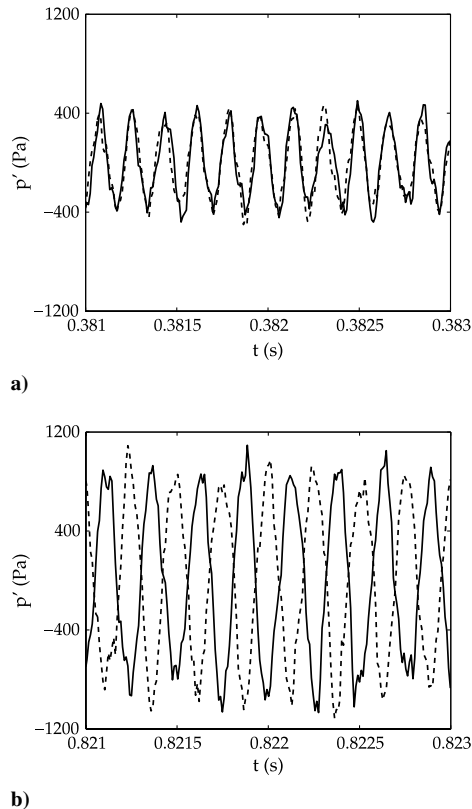


**Fig. 1** Time signals in seconds of pressure (in pascals) recorded by the two near-field microphones: a) NPR = 2.27 and b) NPR = 2.54.

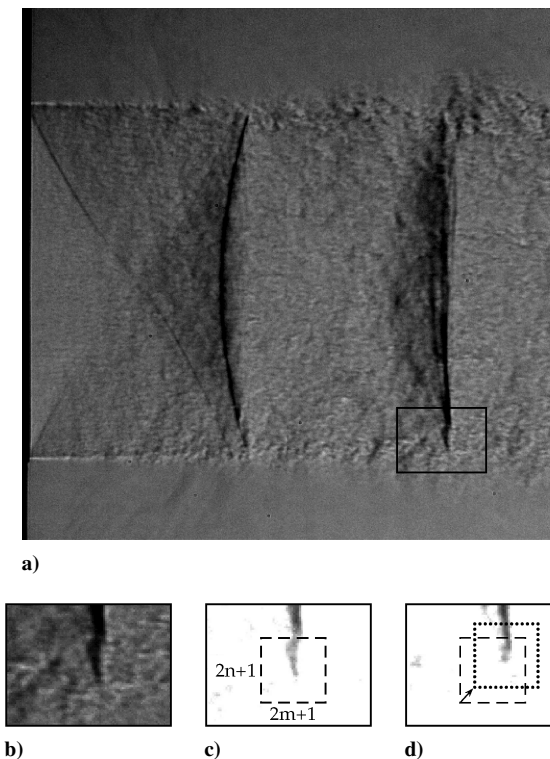


**Fig. 2** Sketch of the shock-tracking algorithm: a) global untreated view of the jet, b) focus on the box about the lower tip of the second shock, considered as referent frame, (c) treated reference frame with the dashed box highlighting the reference patch of size  $(2n + 1) \times (2m + 1)$  px<sup>2</sup>, and d) treated subsequent frame with the dotted box highlighting the computed new position of the selected reference patch whose old position is displayed by the dashed box.

Fig. 2. Shocks are easily located because they are much darker, i.e., they have a lower pixel intensity value in the schlieren pictures than the surrounding medium. Consequently, it was chosen to highlight them by introducing a threshold above which the pixel intensity value is set to 255, or white for these 8-bit images (see Figs. 2b and 2c). In doing so, the intensity value fluctuations caused by turbulence are discarded and shock features are enhanced. The algorithm is then applied on the treated pictures. It was seen that this procedure gave much better results than without pretreatment. The algorithm is taken from Kegerise and Settles [14] and aims at computing an error indicator between a patch chosen in a reference image and any window of same size as the patch in any subsequent frame, expressed as

$$E(i_0, j_0, \Delta i, \Delta j) = \sum_{\delta i=-n}^n \sum_{\delta j=-m}^m [g_1(i_0 + \delta i, j_0 + \delta j) - g_2(i_0 + \delta i + \Delta i, j_0 + \delta j + \Delta j)]^2 \quad (1)$$

where  $E$  is the error estimation between the reference image of 2-D intensity function  $g_1$  and any of the subsequent images of grayscale map  $g_2$ . The pair  $(i_0, j_0)$  are the coordinates of the selected reference point, centered on a distinct shock pattern whose motion one seeks to determine. The reference patch is a  $(2n + 1) \times (2m + 1)$  pixel<sup>2</sup> window centered on  $(i_0, j_0)$ . The error between this reference patch and any patch of same size moving in a window of candidates for the new position of  $(i_0, j_0)$  is computed after (1) with  $\Delta i \in [-N, N]$  and  $\Delta j \in [-M, M]$ . The minimum of the error indicator  $E$  gives the best match in the subsequent picture for the chosen patch. Repeating the procedure for all images in a data set permits following the reference patch in its motion. Results for patches located on either tip of the two first shocks of the jet plume are given here.

First, the frequency of the oscillation is investigated. Power spectral densities (PSDs) of the axial position of selected points on shocks have been computed and all of them display a very strong peak at a frequency very near the screech frequency. The PSD of the axial location of the first shock tip in the NPR = 2.27 case is displayed in Fig. 3 along with the PSD of one simultaneous near-field microphone signal. Both peak at a frequency of 5659 Hz ( $\pm 0.5$  Hz). These results confirm that the shocks oscillate at the screech frequency.

Second, an attempt is made to quantitatively assess the oscillation amplitude. Knowing the oscillation frequency of shocks permits phase averaging to be performed as follows. The first image of each schlieren recording arbitrarily defines the 0° phase. Each schlieren image phase is then computed knowing the time delay from the first image and the oscillation frequency. For the results presented here, images whose phase lies within 1° around the selected values have been averaged, which enhances the shock features even further and builds a more favorable frame to apply the tracking algorithm. The schlieren videos last about 1.08 s, corresponding to approximately 21,600 images.

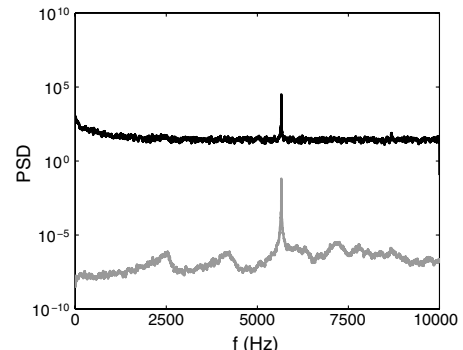


**Fig. 3** Power spectral density of one near-field microphone signal (gray) and PSD  $\times 10^5$  of the signal containing the axial locations of the first shock tip of the NPR = 2.27 case (black). Both spectra have been smoothed away from the peak frequency.

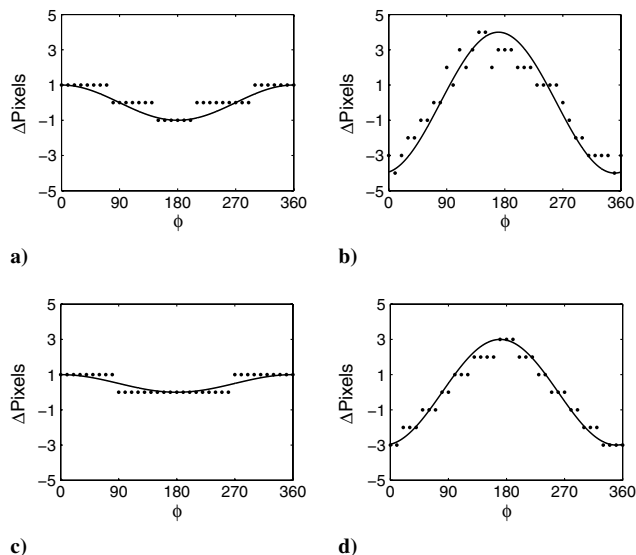


**Fig. 4** Axial position of shock ends in pixels against phase  $\phi$  for the NPR = 2.27 case: a) upper tip of the first shock, b) upper tip of the second shock, c) lower tip of the first shock, and d) lower tip of the second shock; shock positions as provided by the algorithm (dots) and sinusoidal fit through the measured positions (solid line).

The procedure has been used in the NPR = 2.27 case and the results are shown in Fig. 4. The axial motions of the tips of shocks 1 and 2 are found, as expected, to be sinusoidal. In this case, around 60 images have been averaged for each phase. For the displayed results, the computed positions of the shocks have been visually checked on each of the 36 selected phase-averaged images (from 0 to 350° every 10°), and no location error has ever been seen to occur. It has been noted that the lower tips of all shocks oscillated less than the upper tips. It is believed that this arises from non-perfectly-axisymmetric initial conditions of the jet. Two conclusions can readily be drawn:

1) The shocks oscillate in a manner dictated by the screech mode, since mode A is symmetric and so is the shock motion about the jet centerline.

2) The second shock oscillation amplitude is much larger than that of the first shock, whose motion is barely noticeable at this NPR. From about 1 pixel for the first shock, the oscillation amplitude goes up to about 7 pixels for the second one.

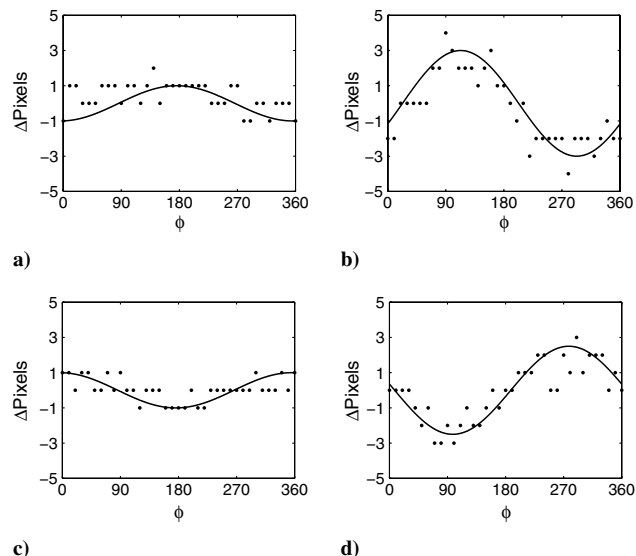


**Fig. 5** Position of second shock ends in pixels against phase  $\phi$  at NPR = 2.54: a) upper tip and weak screech, b) upper tip and strong screech, c) lower tip and weak screech, and d) lower tip and strong screech; shock positions as provided by the algorithm (dots) and sinusoidal fit through the measured positions (solid line).

**Table 1** Amplitude of measured shock oscillations  $\delta_s$  against SPL<sub>s</sub> and shock number<sup>a</sup>

NPR	SPL <sub>s</sub> , dB	Shock	$\delta_s$ , mm	$\delta_s/D$
Mode A				
2.27	144	First	$\approx 0.2$	$\approx 0.005$
2.27	144	Second	$\approx 0.8$	$\approx 0.02$
Mode B				
2.54	139	Second	$\approx 0.3$	$\approx 0.008$
2.54	148	Second	$\approx 0.8$	$\approx 0.02$

<sup>a</sup>SPL<sub>s</sub> is the sound pressure level for screech, and  $D$  is the nozzle diameter.

The tracking procedure has also been applied to a NPR = 2.54 antisymmetric case, whose screech frequency is 3942 Hz. For time intervals larger than that considered in Fig. 1, the near-field acoustic measurements show that the strength of mode B is highly modulated in time. This is in accordance with existing data, e.g., Davies and Oldfield [5]. This feature allows the relationship between screech strength and shock motion magnitude to be pinpointed. The screech amplitude modulation is responsible for the near-field screech level to switch irregularly between about 139 and 148 dB. Since the acoustic data have been acquired in a synchronized manner with the schlieren videos, it has been possible to extract spells of weak and strong screech according to the microphone outputs and to work separately on the corresponding schlieren images. Two sets of images have thus been built, in which the same phase averaging and tracking procedure as for mode A have been applied. Some amplitude results are displayed in Fig. 5. Because of the smaller image subsets, about 12 to 20 images have been averaged for each phase, and so the signal over noise ratio is less than that of Fig. 4. Here again, two conclusions may be drawn:

1) The shock oscillations are in accordance with the screech mode, since mode B is antisymmetric like the shock motion.

2) Shock motion magnitude is clearly related to screech amplitude. From about 2 pixels in weak screech spells, the oscillation amplitude goes up to about 7 pixels in strong screech spells. The latter point, along with the coincidence of the oscillation frequency with screech frequency, might be considered as a proof that screech forces the jet in which it occurs.

The presented results are collected in Table 1. In comparing the results for the second shock of mode A and mode B under strong screech conditions, it is noted that in both cases, oscillation amplitudes are 0.8 mm. However, screech was less strong in mode A recordings than it was for mode B. It is possible that mode A has a greater tendency to oscillate than mode B, in the hypothetical case in which the screech conditions would be equal.

The reported results for mode A of screech are compared with Panda's [13] measured amplitudes for the axisymmetric screech mode at NPR = 2.39. Panda found an amplitude four times as large as the one measured here for the first shock and thrice as large for the second one. Possible reasons for this discrepancy can be a difference in the screech level, which seems to be higher in Panda's case, and the greater NPR considered in his study.

#### IV. Conclusions

A pattern-tracking procedure has been developed to follow shock oscillations in a jet plume under screech condition. This procedure includes treatment of the raw schlieren images and the use of an existing pattern-matching algorithm. Near-field pressure measurements have also been performed in order to link screech properties to shock oscillations. The following have been consistently observed:

- 1) The oscillation frequency of shocks is equal to that of screech.
- 2) The mode of oscillation of shocks, symmetric or antisymmetric, is the same as the screech mode.
- 3) The motion magnitude is an increasing function of the screech amplitude.
- 4) The relation between screech amplitude and shock oscillation magnitude is peculiar to each screech mode.

The presented procedure suffers from some limitations. At first, the triggering of the camera not being conditioned by the microphone output does not permit screech instabilities to be followed. It is assumed here that the screech frequency is perfectly stable, which it is not. This can be seen on the near-field acoustic spectra. They sometimes do not exhibit a perfectly marked peak. This raises the question of the frequency to consider for phase averaging and can lead to lower quality of the averaged pictures. Mode B is less stable than mode A, and this is probably the main reason why the motions for  $\text{NPR} = 2.54$  are not as clear as for  $\text{NPR} = 2.27$ . Furthermore, another optical arrangement could be of interest to increase the resolution of the schlieren images, thus permitting a more precise assessment of oscillation amplitudes.

Despite these caveats, the present study shows that some quantitative results can be achieved from schlieren measurements of jets and confirms the great impact of screech on a jet behavior.

### Acknowledgments

The authors wish to thank Emmanuel Jondeau, Jean-Michel Perrin, and Pascal Souchotte for their technical assistance in setting up the experiments.

### References

- [1] Powell, A., "On the Mechanism of Choked Jet Noise," *Proceedings of the Physical Society of London*, Vol. 66, No. 408, 1953, pp. 1039–1056. doi:10.1088/0370-1301/66/12/306
- [2] Martlew, D. L., "Noise Associated with Shock Waves in Supersonic Jets," AGARD CP 42, Neuilly-sur-Seine, France, 1969, pp. 7-1–7-10.
- [3] Harper-Bourne, M., and Fisher, M. J., "The Noise from Shock Waves in Supersonic Jets," AGARD CP 131, Neuilly-sur-Seine, France, 1973, pp. 11-1–11-13.
- [4] Seiner, J. M., "Advances in High Speed Jet Aeroacoustics," AIAA Paper 84-2275, 1984.
- [5] Davies, M. G., and Oldfield, D. E. S., "Tones From A Choked Axisymmetric Jet. II. The Self Excited Loop and Mode of Oscillation," *Acustica*, Vol. 12, No. 4, 1962, pp. 267–277.
- [6] Merle, M., "Sur la Fréquence des Ondes Émises par un Jet d'Air à Grande Vitesse," *Compte-Rendu de l'Académie des Sciences de Paris*, Vol. 243, 1956, pp. 490–493.
- [7] Powell, A., Umeda, Y., and Ishii, R., "Observations of the Oscillation Modes of Choked Circular Jets," *Journal of the Acoustical Society of America*, Vol. 92, No. 5, 1992, pp. 2823–2836. doi:10.1121/1.404398
- [8] Raman, G., "Advances in Understanding Supersonic Jet Screech: Review and Perspective," *Progress in Aerospace Sciences*, Vol. 34, Nos. 1–2, 1998, pp. 45–106. doi:10.1016/S0376-0421(98)00002-5
- [9] Raman, G., "Supersonic Jet Screech: Half-Century from Powell to the Present," *Journal of Sound and Vibration*, Vol. 225, No. 3, 1999, pp. 543–571. doi:10.1006/jsvi.1999.2181
- [10] Lassiter, L. W., and Hubbard, H. H., "The Near Noise Field of Static Jets and Some Model Studies of Devices for Noise Reduction," NACA TR 1261, 1956.
- [11] Sherman, P. M., Glass, D. R., and Duleep, K. G., "Jet Flow Field During Screech," *Applied Scientific Research*, Vol. 32, No. 3, 1976, pp. 283–303. doi:10.1007/BF00411780
- [12] Panda, J., "A Shock Detection Technique Based on Light Scattering by Shock," *AIAA Journal*, Vol. 33, No. 12, 1995, pp. 2431–2433. doi:10.2514/3.12843
- [13] Panda, J., "Shock Oscillation in Underexpanded Screeching Jets," *Journal of Fluid Mechanics*, Vol. 363, 1998, pp. 173–198. doi:10.1017/S0022112098008842
- [14] Kegerise, M. A., and Settles, G. S., "Schlieren Image-Correlation Velocimetry and Its Application to Free-Convection Flows," *9th International Symposium on Flow Visualization*, Edinburgh, Scotland, U.K., 2000.

D. Papamoschou  
Associate Editor